A simple nonlinear model for the return to isotropy in turbulence

Sutanu Sarkar and Charles G. Speziale
Institute for Computer Applications in Science and Engineering, NASA Langley Research Center, Hampton, Virginia 23665

(Received 31 May 1989; accepted 6 September 1989)

A quadratic nonlinear generalization of the linear Rotta model for the slow pressure-strain correlation of turbulence is developed for high Reynolds number flows. The model is shown to satisfy realizability and to give rise to no stable nonzero equilibrium solutions for the anisotropy tensor in the case of vanishing mean velocity gradients. In order for any model to predict a return to isotropy for all relaxational flows, it is necessary to ensure that there is no nonzero stable fixed point that attracts realizable initial conditions. Both the phase space dynamics and the temporal behavior of the model are examined and compared against experimental data for the return to isotropy problem. It is demonstrated that the quadratic model successfully captures the experimental trends which clearly exhibit nonlinear behavior. Comparisons are also made with the predictions of the linear Rotta model, the quasilinear Lumley model, and the nonlinear model of Shih, Mansour, and Moin. The simple quadratic model proposed in this study does better than the Rotta model as anticipated, and also compares quite favorably with the other more complicated nonlinear models.

I. INTRODUCTION

The *return to isotropy* problem in turbulence has served as a cornerstone for the calibration of models for the slow pressure-strain correlation. The slow pressure-strain correlation is the part of the pressure-strain term that is independent of the mean velocity gradients. It is experimentally observed that an initially anisotropic, homogeneous turbulence produced by the application of constant mean velocity gradients undergoes a relaxation to a state of isotropy when the mean velocity gradients are removed. Rotta[1] was the first to develop a turbulence model for the slow pressure-strain correlation which captured the return to isotropy behavior within the framework of second-order closure models. While the model (which is linear in the anisotropy tensor) performs reasonably well for small initial anisotropies, it can give rise to considerable errors for more general turbulent flows undergoing a relaxation from an initial state that is strongly anisotropic. This was pointed out by Lumley,[2] who emphasized the need to incorporate nonlinear effects and developed a general nonlinear representation for the slow pressure-strain correlation based on invariant tensor representation theory. Subsequent experiments (see Gence and Mathieu[3] and Choi and Lumley[4]) have unequivocally confirmed the nonlinear nature of the return to isotropy problem.

In this paper, a quadratic model for the slow pressure-strain correlation, which contains only one independent constant, will be derived and calibrated. It will be demonstrated that this simple nonlinear model provides for a better description of the return to isotropy problem at high Reynolds numbers than either the linear Rotta model,[1] the quasilinear model[2,5] of Lumley (where nonlinearity is introduced through the invariants of the anisotropy tensor), and the nonlinear model of Shih, Mansour, and Moin.[6] In addition to doing a fairly good job in matching the results of four independent sets of experimental data, the quadratic model will be shown to satisfy realizability and to possess no stable nonzero fixed points in the anisotropy invariant map for relaxational turbulent flows. The latter constraint, which appears to have been overlooked in the previous literature on the subject, is a crucial constraint that nonlinear models must satisfy in order to ensure the return to isotropy for all relaxational turbulent flows. The mathematical properties and dynamical performance of the proposed model will be discussed in detail.

II. FORMULATION OF THE PROBLEM

In conventional, second-order turbulence modeling, transport equations for the Reynolds stress tensor $\overline{u_i u_j}$ and dissipation rate ϵ are solved in addition to the Reynolds averaged Navier–Stokes equations for the mean velocity $\bar{U}_i$. The exact transport equation for the Reynolds stress is

$$\partial_t \overline{u_i u_j} + \bar{U}_k (\overline{u_i u_j})_{,k} = P_{ij} - T_{ijk,k} - D_{ij} + \Pi_{ij} , \tag{1}$$

where

$$\begin{aligned} P_{ij} &= -\overline{u_i u_k}\,\bar{U}_{j,k} - \overline{u_j u_k}\,\bar{U}_{i,k} , \\ T_{ijk} &= \overline{u_i u_j u_k} + (1/\rho)(\overline{p u_i}\,\delta_{jk} + \overline{p u_j}\,\delta_{ik}) \\ &\quad - \nu(\overline{u_i u_j})_{,k} , \\ D_{ij} &= 2\nu\,\overline{u_{i,k} u_{j,k}} , \\ \Pi_{ij} &= (1/\rho)\,\overline{p(u_{i,j} + u_{j,i})} , \end{aligned} \tag{2}$$

given that u_i is the fluctuating velocity, p is the fluctuating pressure, ρ is the mass density, and ν is the kinematic viscosity. In (1), P_{ij} is the production, T_{ijk} is the diffusive transport, D_{ij} is the dissipation rate tensor, Π_{ij} is the pressure-strain correlation, an overbar represents an ensemble mean, and a comma denotes a partial derivative with respect to the

 0899-8213/90/010084-10$02.00

spatial coordinates. A transport equation is also usually carried for the dissipation rate ϵ, which is defined as follows

$$\epsilon = \nu \overline{u_{i,j} u_{i,j}} \,. \tag{3}$$

The typical approach to modeling the unknown correlations T_{ijk}, D_{ij}, and Π_{ij} in (1) is to express them as functions of the Reynolds stress tensor $\overline{u_i u_j}$, the gradients of the Reynolds stress tensor $(\overline{u_i u_j})_{,k}$, the mean velocity gradients $\bar{U}_{i,j}$, the dissipation rate ϵ, and the kinematic viscosity ν at lower turbulence Reynolds numbers.

At high Reynolds numbers, the dissipation rate tensor is nearly isotropic so that we can set

$$D_{ij} = \tfrac{2}{3}\epsilon\,\delta_{ij} \,. \tag{4}$$

The quantity Π_{ij} can be decomposed into a slow pressure-strain term Π_{ij}^S which is independent of $\bar{U}_{i,j}$ and a rapid term Π_{ij}^R, which is linear in $\bar{U}_{i,j}$. The dependence of the slow pressure-strain correlation Π_{ij}^S on $\overline{u_i u_j}$ and ϵ can be studied in isolation by considering the *return to isotropy* problem. The return to isotropy problem refers to the flow wherein *homogeneous, anisotropic* turbulence produced by mean velocity gradients is observed to relax toward isotropy when the mean velocity gradients are removed. This return to isotropy problem is an idealized case, but it is important nevertheless because it serves to extract and calibrate a part of the general functional dependence of Π_{ij} for more complex turbulent flows.

Equation (1) for the Reynolds stress tensor simplifies considerably for the return to isotropy of homogeneous turbulence since $\bar{U}_{i,j}$ and $T_{ijk,k}$ are identically zero, and D_{ij} may be assumed to be isotropic at high turbulence Reynolds numbers. The simplified form of (1) is written as follows:

$$\overset{\cdot}{\overline{u_i u_j}} = \Pi_{ij}^S - \tfrac{2}{3}\epsilon\delta_{ij}, \tag{5}$$

where we have made use of the fact that the rapid part of the pressure-strain correlation vanishes for vanishing $\bar{U}_{i,j}$.

The anisotropy tensor b_{ij} is defined by

$$b_{ij} = \overline{u_i u_j}/q^2 - \tfrac{1}{3}\delta_{ij} \,, \tag{6}$$

where

$$q^2 = \overline{u_i u_i} \,. \tag{7}$$

The matrix associated with the anisotropy tensor is denoted by $\mathbf{b}$. Using (5) and its contraction, the following evolution equation for b_{ij} is obtained:

$$\dot{b}_{ij} = \Pi_{ij}^S/q^2 + 2(\epsilon/q^2)b_{ij} \,. \tag{8}$$

If we define a dimensionless tensor Φ_{ij} by

$$\Pi_{ij}^S = -\epsilon\Phi_{ij} \,, \tag{9}$$

(8) can be rewritten as follows:

$$\dot{b}_{ij} = -(\epsilon/q^2)(\Phi_{ij} - 2b_{ij}) \,. \tag{10}$$

Equation (10) must be solved along with evolution equations for q^2 and ϵ. For the return to isotropy problem, the exact transport equation for q^2 and the standard model equation for ϵ are as follows:

$$\begin{aligned} \dot{q}^2 &= -2\epsilon \,, \\ \dot{\epsilon} &= -2C_{\epsilon 2}(\epsilon^2/q^2) \,, \end{aligned} \tag{11}$$

where $C_{\epsilon 2}$ is a constant that assumes a value of approximately 1.90.

The important variables in this homogeneous, high Reynolds number flow are b_{ij}, q^2, and ϵ. Lumley[2] gave the general tensorial form of the function $\Phi_{ij}(b_{ij}, q^2, \epsilon)$, which can be written as follows:

$$\begin{aligned} \Phi_{ij} &= \alpha_1(\mathrm{II}_b, \mathrm{III}_b)b_{ij} + \alpha_2(\mathrm{II}_b, \mathrm{III}_b) \\ &\quad \times [b_{ik}b_{kj} - (\mathrm{II}_b/3)\delta_{ij}] \,. \end{aligned} \tag{12}$$

In (12), α_1 and α_2 are general functions of the invariants $\mathrm{II}_b = b_{ik}b_{ki}$ and $\mathrm{III}_b = b_{ik}b_{kj}b_{ji}$. It should be noted that II_b and III_b denote the traces of $\mathbf{b}^2$ and $\mathbf{b}^3$, respectively, and differ from the principal invariants (II, III) of $\mathbf{b}$ by constant multiplicative factors since $\mathbf{b}$ is traceless. On substituting the model of Φ_{ij} from (12) into (10), we obtain

$$\begin{aligned} \dot{b}_{ij} = &-(\epsilon/q^2)\{[\alpha_1(\mathrm{II}_b, \mathrm{III}_b) - 2]b_{ij} \\ &+ \alpha_2(\mathrm{II}_b, \mathrm{III}_b)[b_{ik}b_{kj} - (\mathrm{II}_b/3)\delta_{ij}]\} \,. \end{aligned} \tag{13}$$

A prescription of the functions $\alpha_1(\mathrm{II}_b, \mathrm{III}_b)$ and $\alpha_2(\mathrm{II}_b, \mathrm{III}_b)$ is now required to close (13). The approach that is most widely used in practice is the linear model proposed by Rotta[1] in which $\alpha_1(\mathrm{II}_b, \mathrm{III}_b)$ is assumed to be a constant and $\alpha_2(\mathrm{II}_b, \mathrm{III}_b)$ is assumed to be zero. The commonly used second-order closure model of Launder, Reece, and Rodi[7] is based on the Rotta model, where

$$\begin{aligned} &\alpha_1(\mathrm{II}_b, \mathrm{III}_b) = C_1 \approx 3.0 \,, \\ &\alpha_2(\mathrm{II}_b, \mathrm{III}_b) = 0 \,. \end{aligned} \tag{14}$$

Lumley and Newman[8] and Lumley[2] have pointed out that experimental data does not support the linear model of Rotta. The problem with the linear model is twofold: (a) its prediction that each component of the anisotropy tensor decays at the same rate; and (b) its prediction that this decay rate is independent of the initial state of anisotropy. These predictions can be seen mathematically in the closed form solution of the return to isotropy problem for the Rotta model, given by

$$b_{ij} = b_{ij}(0)[1 + 2(C_{\epsilon 2} - 1)(\epsilon_0/q_0^2)t]^{-1/2(C_{\epsilon 2} - 1)} \,. \tag{15}$$

In contradiction to (15), experiments indicate that the rate of the return to isotropy *decreases* with increasing values of the third invariant III_b, and that different components of the anisotropy tensor relax to zero at *different* rates. These are effects that are decidedly nonlinear.

In order to incorporate nonlinear effects, Lumley[2] developed a model within the framework of (12), and also allowed the coefficients α_1 and α_2 to additionally depend on the turbulence Reynolds number $\mathrm{Re}_t = q^4/9\epsilon\nu$. This quasi-linear model of Lumley[2] is as follows:

$$\begin{aligned} &\alpha_1(\mathrm{II}_b, \mathrm{III}_b, \mathrm{Re}_t) \\ &\quad = 2.0 + \frac{F}{9}\exp\left(\frac{-7.77}{\sqrt{\mathrm{Re}_t}}\right)\left(\frac{72}{\sqrt{\mathrm{Re}_t}}\right. \\ &\qquad \left. + 80.1\ln[1 + 62.4(-\mathrm{II} + 2.3\mathrm{III})]\right) \,, \end{aligned} \tag{16}$$

$$\alpha_2(\mathrm{II}_b, \mathrm{III}_b, \mathrm{Re}_t) = 0 \,,$$

where

$$F = 1 + 9\mathrm{II} + 27\mathrm{III},$$
$$\mathrm{II} = -\mathrm{II}_b/2, \quad \mathrm{III} = \mathrm{III}_b/3 . \tag{17}$$

Here, we refer to this model as being quasilinear since there is no tensorial nonlinearity, that is,

$$\Phi_{ij} = \alpha_1(\mathrm{II}_b,\mathrm{III}_b,\mathrm{Re}_t)b_{ij} . \tag{18}$$

It will be shown later that while this model does correctly mimic some of the nonlinear effects associated with the return to isotropy (see Shih and Lumley[5]) it yields an incorrect representation of the problem in phase space.

Shih, Mansour, and Moin have recently proposed a nonlinear model for Φ_{ij}, hereafter referred to as the SMM model, which is as follows[6]:

$$\alpha_1(\mathrm{II}_b,\mathrm{III}_b,\mathrm{Re}_t) = 2.0 + \frac{F^{0.85}}{9}\exp\left(\frac{-7.77}{\sqrt{\mathrm{Re}_t}}\right) \times\left(\frac{72}{\sqrt{\mathrm{Re}_t}} + 80.1\ln[1 + 62.4(-\mathrm{II} + 2.3\mathrm{III})]\right) - 2(1 - F^{0.05})\left(\frac{1}{3} + 2\mathrm{II}\right),$$
$$\alpha_2(\mathrm{II}_b,\mathrm{III}_b,\mathrm{Re}_t) = -2(1 - F^{0.05}) , \tag{19}$$

where F, II, and III are as defined previously in (17). We will show later that the SMM model yields predictions for the return to isotropy experiments, which are nearly identical to those of the Lumley model. In the following sections, a quadratic model will be developed, tested against experimental data, and shown to capture the essence of the nonlinearity in phase space.

III. THE QUADRATIC NONLINEAR MODEL

We will now develop a quadratic model, which is a special case of (12). Since each component energy $\overline{u_\alpha u_\alpha}$ (where Greek indices indicate no summation) is bounded by

$$0 \leqslant \overline{u_\alpha u_\alpha} \leqslant q^2 , \tag{20}$$

it is a simple matter to show from (6) that each principal value of b_{ij} (denoted by $b^{(\alpha)}$) lies in the range

$$-\tfrac{1}{3} \leqslant b^{(\alpha)} \leqslant \tfrac{2}{3} . \tag{21}$$

Consequently, the principal values of b_{ij} are less than unity, and it is possible that a lower-order Taylor expansion of $\Phi_{ij}(b_{ij})$ around the isotropic state of $b_{ij} = 0$ can yield an adequate approximation. Carrying out such a Taylor expansion around $b_{ij} = 0$, while constraining Φ_{ij} to be of zero trace, gives

$$\mathbf{\Phi} = C_1\mathbf{b} - C_2[\mathbf{b}^2 - (\mathrm{II}_b/3)\mathbf{I}] + C_3[\mathbf{b}^3 - (\mathrm{III}_b/3)\mathbf{I}] + \cdots , \tag{22}$$

where $C_1, C_2, C_3, \ldots$, are constants. In (22) we use coordinate-free notation, that is, we denote Φ_{ij}, b_{ij}, and δ_{ij} by the associated matrices $\mathbf{\Phi}$, $\mathbf{b}$, and $\mathbf{I}$. Using the Cayley–Hamilton theorem to express $\mathbf{b}^3$ and higher powers of $\mathbf{b}$ in terms of $\mathrm{II}_b, \mathrm{III}_b$, $\mathbf{b}$, and $\mathbf{b}^2$ reduces (22) to (12), where $\alpha_1(\mathrm{II}_b,\mathrm{III}_b)$ and $\alpha_2(\mathrm{II}_b,\mathrm{III}_b)$ are polynomial functions of II_b and III_b of infinite degree.

The model of Φ_{ij} that we propose in this paper is a quadratic truncation of (22), and is given by

$$\Phi_{ij} = C_1 b_{ij} - C_2[b_{ik}b_{kj} - (\mathrm{II}_b/3)\delta_{ij}] , \tag{23}$$

where C_1 and C_2 are constants. Such a quadratic model is attractive because it is the simplest nonlinear model for Φ_{ij} [of course a linear truncation of (22), which leads to Rotta's model, would be even more simple but, unfortunately, is in conflict with experimental data]. Furthermore, since for most problems of engineering interest the magnitude of b_{ij} tends to be less than $\frac{1}{3}$, there is a good chance for a quadratic model to yield an acceptable approximation for a variety of flows.

At this point, we will derive the evolution equations determining the phase space dynamics for the return to isotropy problem. It is useful to introduce the transformed time variable τ defined by

$$d\tau = (\epsilon/q^2)dt , \tag{24}$$

in order to free the formulation of the problem from any explicit dependence on ϵ and q^2. Using the system of equations (11) to solve for $q^2(t)$ and $\epsilon(t)$, and integrating (24), we obtain the following explicit relationship between τ and t:

$$\tau = [1/2(C_{\epsilon 2} - 1)]\ln[1 + 2(C_{\epsilon 2} - 1)(\epsilon_0/q_0^2)t] . \tag{25}$$

Using (24), the transport equation (13) for b_{ij} can then be rewritten as

$$\frac{db_{ij}}{d\tau} = -\left[(\alpha_1(\mathrm{II}_b,\mathrm{III}_b) - 2)b_{ij} + \alpha_2(\mathrm{II}_b,\mathrm{III}_b) \times\left(b_{ik}b_{kj} - \frac{\mathrm{II}_b}{3}\delta_{ij}\right)\right], \tag{26}$$

which is clearly independent of q^2 and ϵ.

We now show that the phase space for (26) is two dimensional. Let the principal axes of b_{ij} at $\tau = 0$ be $\{x_1,x_2,x_3\}$ and the corresponding eigenvalues of b_{ij} be denoted by b_{11}, b_{22}, and b_{33}. The off-diagonal terms, $b_{ij}(i \neq j)$ are zero at $\tau = 0$. Upon examining (26) in principal axes form it is clear that

$$\frac{db_{ij}}{d\tau} = 0 \quad \text{for} \quad i \neq j . \tag{27}$$

Since $b_{ij}(0)$ is zero for $i \neq j$, we conclude from (27) that the off-diagonal terms of b_{ij} are identically zero for all times; and therefore the principal axes of b_{ij} do not change in time. The time invariance of the principal axes has been experimentally observed, for example, by Gence and Mathieu.[3] Therefore the only time varying components of b_{ij}, referred to the coordinate system $\{x_1,x_2,x_3\}$, are b_{11}, b_{22}, and b_{33}. Since b_{ij} is traceless, only two of the three quantities b_{11}, b_{22}, and b_{33}, are independent. Thus the phase space in this problem is two dimensional. The two phase space variables may be chosen to be any two independent functions of the eigenvalues of b_{ij}.

A possible choice for phase space variables is II_b and III_b. The variables II_b and III_b are desirable to use since they are uniquely determined by the principal values of b_{ij}, are invariant to a rotation of coordinates, and vanish in isotropic turbulence. Furthermore, because $\mathrm{II}_b \geqslant 0$ the phase space becomes semi-infinite in the variable II_b. The evolution equa-

tions for $II_b(\tau)$ and $III_b(\tau)$ will now be derived. Multiplying (26) by b_{ij} and $b_{ik}b_{kj}$, respectively, we obtain the following equations:

$$\frac{dII_b}{d\tau} = -2[(\alpha_1 - 2)II_b + \alpha_2 III_b], \tag{28}$$

$$\frac{dIII_b}{d\tau} = -3\left[(\alpha_1 - 2)III_b + \alpha_2\left(\mathrm{tr}(\mathbf{b}^4) - \frac{II_b^2}{3}\right)\right]. \tag{29}$$

In (29), $\mathrm{tr}(\mathbf{b}^4)$ denotes the trace of the tensor $\mathbf{b}^4$. Using the Cayley–Hamiltonian theorem, it follows that

$$\mathbf{b}^4 = \tfrac{1}{2}II_b\mathbf{b}^2 + (III_b/3)\mathbf{b}. \tag{30}$$

By taking the trace of (30), and substituting the results into (29), we obtain

$$\frac{dIII_b}{d\tau} = -3\left[(\alpha_1 - 2)III_b + \alpha_2\frac{II_b^2}{6}\right]. \tag{31}$$

Equations (28) and (31) constitute a coupled nonlinear system of ordinary differential equations for $II_b(\tau)$ and $III_b(\tau)$.

Both the Rotta model (14) and the Lumley model (16) choose $\alpha_2 = 0$. When $\alpha_2 = 0$, (28) and (31) can be combined and integrated to yield the general solution

$$(II_b)^{1/2} = c(III_b)^{1/3}, \tag{32}$$

where c is a constant of integration determined by initial conditions. In terms of the variables

$$\xi = (III_b)^{1/3}, \qquad \eta = (II_b)^{1/2}, \tag{33}$$

which were first introduced by Choi and Lumley,[4] (32) takes the linear form

$$\eta/\eta_0 = \xi/\xi_0. \tag{34}$$

These alternative variables have the advantage that in the ξ-η phase space both the linear and quasilinear models show *straight line* trajectories. Therefore both the linear Rotta model and quasilinear Lumley model always display straight line trajectories in ξ-η phase space. Some of the experimental data that will be shown later exhibit *curved* trajectories in ξ-η phase space which constitutes conclusive evidence in support of the need for nonlinear models wherein both α_1 and α_2 are nonzero.

In Fig. 1 we show the *anisotropy invariant map* that denotes the realizable portion of phase space in which turbulence exists. Turbulence is constrained to lie in the region ABC bounded by the two straight line segments AB and AC representing axisymmetric turbulence and the curved line BC denoting two-dimensional (2-D) turbulence. Point A corresponds to isotropic turbulence and point B corresponds to the 1-D turbulent state.

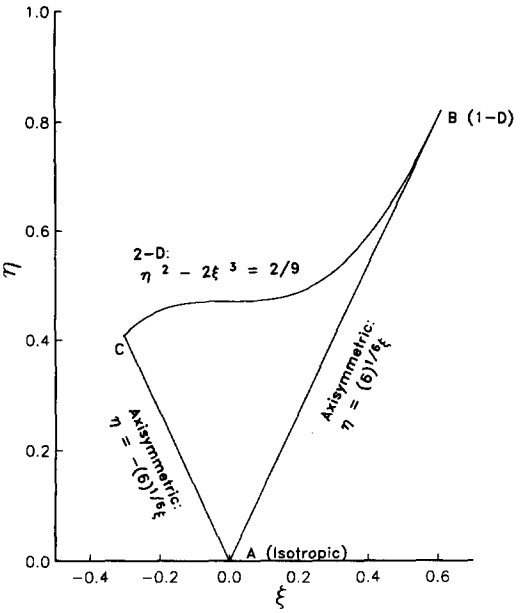

FIG. 1. The anisotropy invariant map in ξ-η phase space.

IV. FIXED POINT ANALYSIS IN PHASE SPACE

A fixed point analysis of the quadratic model in the phase space of the invariants of b_{ij} will now be presented. The fixed points of (28) and (31) (where, for the simple quadratic model, $\alpha_1 = C_1$ and $\alpha_2 = -C_2$) are the equilibrium solutions in the limit $\tau \to \infty$, which are denoted by $(II_b)_\infty, (III_b)_\infty$. If the turbulence is to return to isotropy,

$$(II_b)_\infty = (III_b)_\infty = 0. \tag{35}$$

Therefore, since physical and numerical experiments indicate that any initial anisotropy which is realizable tends to relax to zero when the mean velocity gradients are removed, it is essential that nonlinear models for the slow pressure-strain correlation have *no stable fixed points* other than (0,0) which lie in the anisotropy invariant map.

Since the linear model (for which $C_2 = 0$) gives rise to the following system of evolution equations:

$$\frac{dII_b}{d\tau} = -2(C_1 - 2)II_b, \qquad \frac{dIII_b}{d\tau} = -3(C_1 - 2)III_b, \tag{36}$$

it is a simple matter to show that (0,0) is the only fixed point, and that it is a stable node, provided that $C_1 > 2$.

We now examine the existence and stability of the fixed points predicted by our quadratic model (23). The quadratic model leads to the following equations for $II_b(\tau)$ and $III_b(\tau)$:

$$\frac{dII_b}{d\tau} = -2(C_1 - 2)II_b + 2C_2 III_b, \qquad \frac{dIII_b}{d\tau} = -3(C_1 - 2)III_b + \frac{C_2}{2}II_b^2. \tag{37}$$

The fixed points of the system (37) are solutions of the nonlinear algebraic equations obtained by setting $dII_b/d\tau = dIII_b/d\tau = 0$, and are given by

$$(II_b)_\infty = 0, \quad (III_b)_\infty = 0, \tag{38}$$

$$(II_b)_\infty = 6\beta^2, \quad (III_b)_\infty = 6\beta^3, \tag{39}$$

where $\beta = (C_1 - 2)/C_2$.

In order to examine the stability of these fixed points we introduce the new variables (z_1,z_2) defined by

$$z_1 = \mathrm{II}_b - (\mathrm{II}_b)_\infty , \quad z_2 = \mathrm{III}_b - (\mathrm{III}_b)_\infty . \tag{40}$$

If we substitute (40) into (37), and retain only the terms that are linear in z_1 and z_2, we obtain the following linear system of ordinary differential equations:

$$\frac{dz_i}{d\tau} = A_{ij} z_j , \tag{41}$$

where A_{ij} is the following matrix:

$$\begin{bmatrix} -2(C_1-2) & 2C_2 \\ C_2(\mathrm{II}_b)_\infty & -3(C_1-2) \end{bmatrix}.$$

The eigenvalues of A_{ij} determine the stability of the fixed points. A fixed point is stable if all the eigenvalues of A_{ij} are negative. The fixed point (0,0) has eigenvalues $A^{(\alpha)}$ given by

$$A^{(1)} = -2(C_1-2), \quad A^{(2)} = -3(C_1-2) \tag{42}$$

and hence is a stable node, provided that

$$C_1 > 2 . \tag{43}$$

On the other hand, the fixed point $(6\beta^2, 6\beta^3)$ has the eigenvalues

$$A^{(1)} = C_1 - 2, \quad A^{(2)} = -6(C_1-2) . \tag{44}$$

Since the eigenvalues are of opposite sign no matter what value is taken for C_1, the fixed point $(6\beta^2, 6\beta^3)$ is a saddle which is *unstable*. It is thus clear that $(\mathrm{III}_b)_\infty = (\mathrm{II}_b)_\infty = 0$ is the only stable equilibrium solution. It may be noted that the locus of the saddle point given by (39) corresponds (in Fig. 1) to the straight line containing AC and the straight line containing AB extended to infinity. Thus any axisymmetric state of turbulence is a possible location for the saddle point of the quadratic model.

V. CONSTRAINTS ON THE MODEL CONSTANTS

The quadratic model has two constants C_1 and C_2 which, for the purpose of stability, need only satisfy the constraint $C_1 > 2$. We will now explore whether there are additional physical constraints on the range of allowable values of C_1 and C_2. Choi and Lumley[4] and Le Penven, Gence, and Comte-Bellot[9] have analyzed available sets of experimental data (approximately 10 in number) on the relaxation of anisotropic turbulence. They conclude from the data that a characteristic nondimensional time rate for the relaxation [defined by $-(1/\mathrm{II}_b)(d\,\mathrm{II}_b/d\tau)$] *decreases* with increasing values of III_b. An examination of (37) shows that in order for the model to reproduce this trend we must choose

$$C_2 > 0. \tag{45}$$

Since $C_1 > 2$ and $C_2 > 0$, according to (39) the saddle point of the quadratic model lies on the line containing AB in Fig. 1, extended to infinity. Furthermore, it can be shown that the unstable manifold of the saddle point is tangent to the line AB. Trajectories diverge away from the saddle either toward the isotropic state or toward the unrealizable region of the ξ-η phase space. In order to ensure that all realizable states of turbulence return to isotropy, it follows that the saddle point cannot be placed on the portion of line AB that is below point B. Thus the η coordinate of the saddle point must not be smaller than $(\frac{2}{9})^{1/2}$, and from (39) it follows that

$$C_2 \leqslant 3(C_1 - 2) . \tag{46}$$

Lumley[2] uses the concept of realizability, which requires that model predictions satisfy all moment inequalities; for example, the model is required to yield non-negative component energies. Lumley's method leads to various equations relating the model constants. Pope[10] suggests that a related but weaker mathematical statement, which constitutes a sufficient condition to guarantee non-negative component energies, should be used. The application of both approaches in the context of the quadratic model for Φ_{ij} will now be discussed.

The transport equations for b_{ij} and $\overline{u_i u_j}$ in the present problem are

$$\dot{b}_{ij} = -(\epsilon/q^2)(\Phi_{ij} - 2b_{ij}) , \tag{47}$$

$$\dot{\overline{u_i u_j}} = -\epsilon\Phi_{ij} - \tfrac{2}{3}\epsilon\,\delta_{ij} . \tag{48}$$

The three eigenvalues of $\overline{u_i u_j}$ are the three components in the principal axes of $\overline{u_i u_j}$; these components are $\overline{u_1^2}$, $\overline{u_2^2}$, and $\overline{u_3^2}$. Consider one of the eigenvalues, for example, $\overline{u_1^2}$. Realizability requires that

$$\overline{u_1^2} \geqslant 0. \tag{49}$$

Using the Lumley[2] approach to satisfy realizability leads to the requirement that

$$\dot{\overline{u_1^2}} = 0 \quad \text{when} \quad \overline{u_1^2} = 0 , \tag{50}$$

whereas the Pope[10] approach leads to the requirement that

$$\dot{\overline{u_1^2}} \geqslant 0 \quad \text{when} \quad \overline{u_1^2} = 0 . \tag{51}$$

Both approaches guarantee that the realizability condition (49) is satisfied. However, (51) can prevent $\overline{u_1^2}$ from ever becoming zero (which is the physically realizable limit of two-dimensional turbulence), and hence is more conservative than (50) in this regard. But since (51) does guarantee positive component energies, we will be content for the moment to consider it since it places less restrictions on C_1 and C_2.

Since (51) is to be satisfied using (48), we require that

$$-\epsilon\phi_{11} - \tfrac{2}{3}\epsilon \geqslant 0 \quad \text{when} \quad \overline{u_1^2} = 0. \tag{52}$$

This implies that

$$\phi_{11} \leqslant -\tfrac{2}{3} \quad \text{when} \quad \overline{u_1^2} = 0. \tag{53}$$

Substituting the quadratic model for Φ_{ij} from (23) into (53) leads to the inequality

$$C_1 b_{11} - C_2(b_{11}^2 - \mathrm{II}_b/3) \leqslant -\tfrac{2}{3} \quad \text{when} \quad \overline{u_1^2} = 0. \tag{54}$$

Since $b_{11} = -\frac{1}{3}$ when $\overline{u_1^2} = 0$, (54) becomes

$$C_1 - 2 \geqslant C_2(\mathrm{II}_b - \tfrac{1}{3}) . \tag{55}$$

Equation (55) must be satisfied for any allowable value of II_b. From the constraint (43), it is clear that the left-hand side of (55) is positive. Since from (45) $C_2 > 0$, the maximum value of the right-hand side of (55) occurs when II_b is at its maximum value. Therefore a sufficient condition for

satisfying (55) is obtained when II_b is equal to its maximum value $(II_b)_{max}$. It can be easily shown that

$$(II_b)_{max} = \tfrac{2}{3}. \tag{56}$$

By substituting the maximum value of II_b, which is given by (56), into (55), we obtain the following constraint:

$$C_2 \leqslant 3(C_1 - 2), \tag{57}$$

which is identical to the constraint (46), which had been derived earlier based on a different argument. Thus, interestingly enough, both realizability and dynamical systems arguments lead to the same model constraint. For a given value of C_1, (57) determines the maximum allowable value of C_2.

VI. MODEL PERFORMANCE

The coupled system of nonlinear ordinary differential equations (28) and (31) were numerically integrated by a Runge–Kutta method to obtain $II_b(\tau)$ and $III_b(\tau)$. The initial conditions corresponding to those of the previously conducted experiments were used. The phase plots in ξ-η space and the transient plots of $II_b(\tau)$ and $III_b(\tau)$ were the yardsticks by which the model results and experimental data were compared.

We recall that the proposed model for the slow pressure-strain correlation is as follows:

$$\Pi_{ij}^S = -\epsilon\{C_1 b_{ij} - C_2[b_{ik}b_{kj} - (II_b/3)\delta_{ij}]\}. \tag{58}$$

Phase plots in ξ-η space and transient plots of $II_b(\tau)$ and $III_b(\tau)$ were obtained for various choices of the constants C_1 and C_2 in our model, and compared with available experimental data. A numerical optimization showed that for a given value of C_1 it was best to choose the maximum value of C_2 allowed by (57), that is, to set

$$C_2 = 3(C_1 - 2). \tag{59}$$

As a result of (59), C_2 is uniquely determined by C_1 making the model one with a *single* free constant C_1. The following choice of the one independent model constant:

$$C_1 = 3.4, \tag{60}$$

which according to (59) gives $C_2 = 4.2$, seems to best reflect the experimental data.

Results on the performance of the linear Rotta model, the quasilinear Lumley model, the nonlinear SMM model, and the present quadratic model are compared with four sets of experimental data in Figs. 2–13. Figures 2–4 consider the plane distortion experiment of Choi and Lumley.[4] The experimental data in Fig. 2 shows strong nonlinearity in the ξ-η phase plane (as demonstrated by a curved trajectory), which is reproduced by the quadratic model. However, the trajectories in the ξ-η phase space of the Rotta and Lumley models are identical and are always straight lines, which is in serious disagreement with this experimental data. The SMM model, though formally nonlinear, has a phase space trajectory in Fig. 2 which is nearly identical to those of the Rotta and Lumley models. The reason for this lies in the fact that the coefficient α_2 for the SMM model, as defined in (19), is insignificant compared to α_1 for this data set. In fact, the quadratic term is negligible compared to the linear term in the SMM model for $F > 0.2$. It is only when the turbulence is

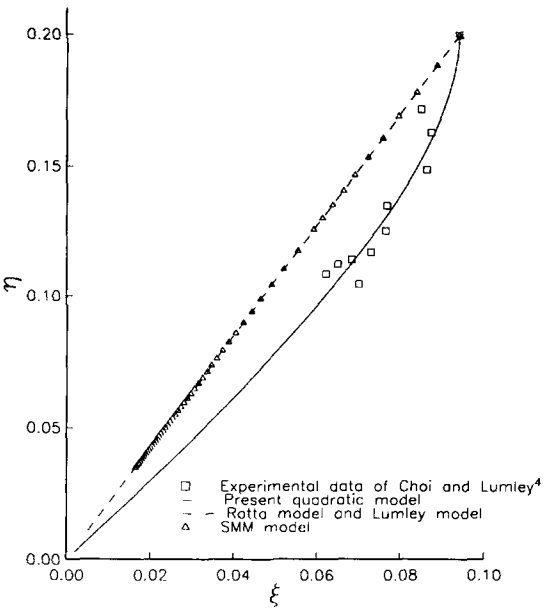

FIG. 2. A phase space comparison of the model predictions with the plane distortion experiment of Choi and Lumley.[4]

somewhat close to the 2-D state, for which $F = 0$, that the value of the quadratic term in the SMM model becomes large enough to cause significant nonlinearity in the ξ-η phase trajectories. All of the return to isotropy experiments consider turbulence far removed from the 2-D state: therefore the phase space trajectories for the SMM model and the Lumley model are not only approximately the same in Fig. 2, but also for the other experiments considered in this study. Furthermore, since the effective values of α_1 for the SMM model and the Lumley model are approximately the same for these experiments, the temporal evolution of II_b and III_b are nearly identical for these two models. Figures 3 and 4 show the

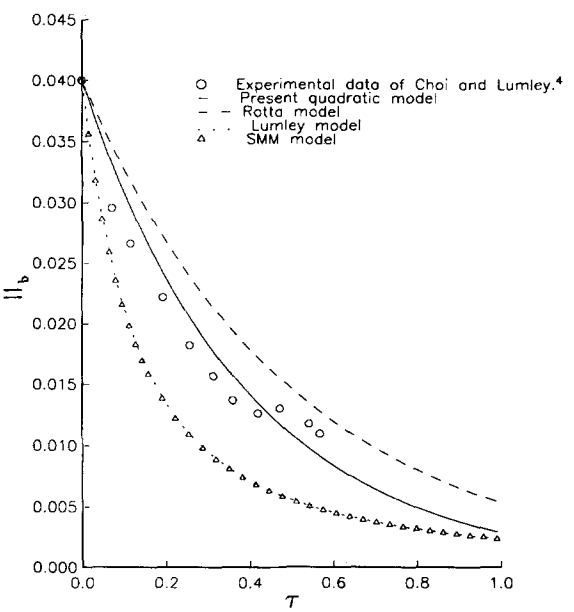

FIG. 3. Temporal decay of the second invariant of the anisotropy tensor: comparison of the model predictions with the plane distortion experiment of Choi and Lumley.[4]

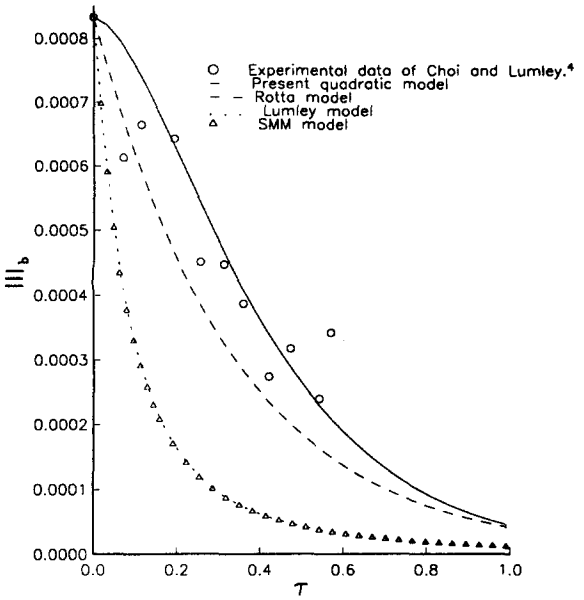

FIG. 4. Temporal decay of the third invariant of the anisotropy tensor: comparison of the model predictions with the plane distortion experiment of Choi and Lumley.[4]

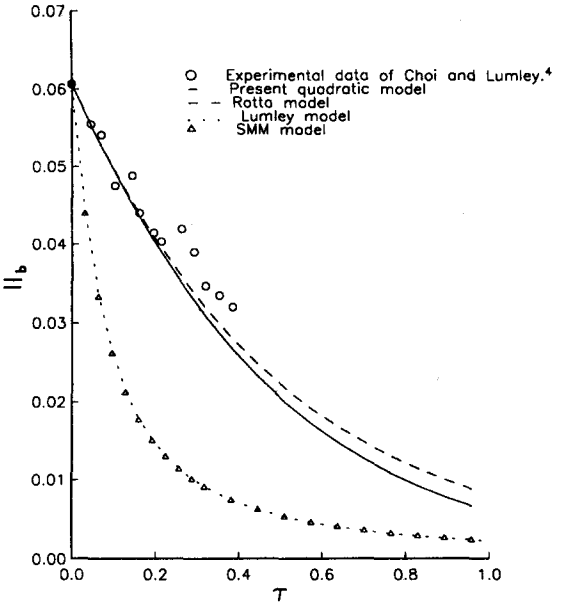

FIG. 6. Temporal decay of the second invariant of the anisotropy tensor: comparison of the model predictions with the axisymmetric expansion experiment of Choi and Lumley.[4]

temporal behavior of II_b and III_b. It is seen that the present quadratic model is superior to both the Rotta model and the Lumley model with regard to capturing the temporal behavior of both II_b and III_b.

Figures 5–7 pertain to the axisymmetric expansion experiment of Choi and Lumley.[4] The experimental phase space trajectory seems to be fairly linear as shown in Fig. 5, and the present quadratic model also shows nearly linear behavior. Apparently, the quadratic model not only shows nonlinear trajectories in ξ-η phase space when called for, but also gives rise to approximately linear trajectories in the appropriate region of phase space where nonlinear effects are small. It is seen in Figs. 6 and 7 that the results of both the Rotta model and the quadratic model on the temporal behavior of II_b and III_b are in reasonable agreement with the experimental data; however, the Lumley model and the SMM model predict a decay rate that is much more rapid than the experimentally observed result.

Le Penven *et al.*[9] used two different plane contractions to generate anisotropic turbulence with positive III_b in one case and negative III_b in the other case. Their experimental data on the relaxation of turbulence with positive III_b is shown in Figs. 8–10. Their data of Fig. 8 indicate a moder-

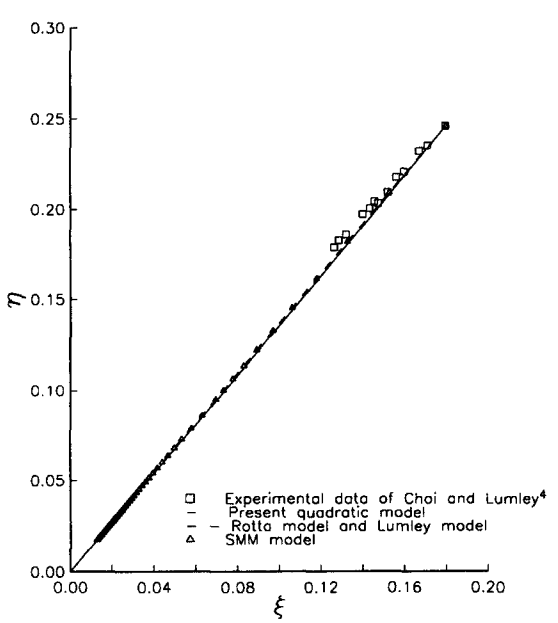

FIG. 5. A phase space comparison of the model predictions with the axisymmetric expansion experiment of Choi and Lumley.[4]

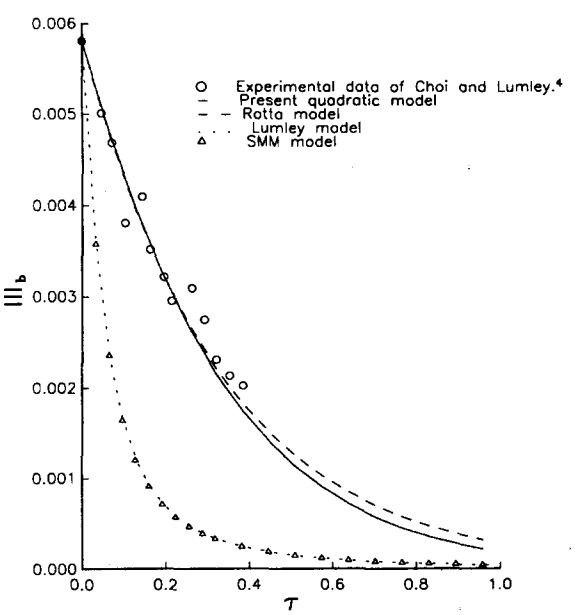

FIG. 7. Temporal decay of the third invariant of the anisotropy tensor: comparison of the model predictions with the axisymmetric expansion experiment of Choi and Lumley.[4]

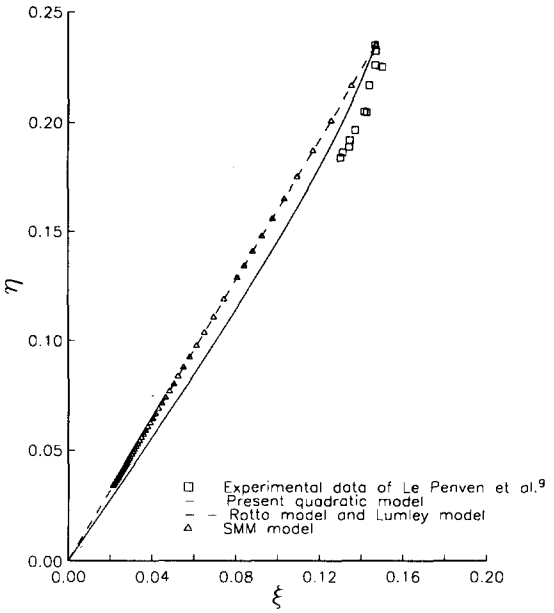

FIG. 8. A phase space comparison of the model predictions with the plane contraction experiment of Le Penven *et al.*[9] for $III_b\ (0) > 0$.

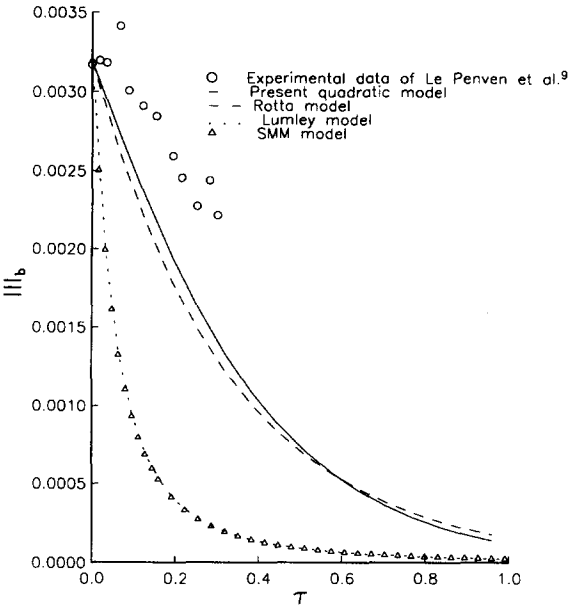

FIG. 10. Temporal decay of the third invariant of the anisotropy tensor: comparison of the model predictions with the plane contraction experiment of Le Penven *et al.*[9] for $III_b(0) > 0$.

ately curved trajectory in phase space, and the quadratic model yields a prediction that is in qualitatively good agreement with the data. Figure 9 shows that the quadratic model does a better job than the Lumley model and the SMM model in predicting the temporal decay of II_b (suprisingly, in this case, the Rotta model is slightly better than the quadratic model with regard to predicting the temporal behavior of II_b). As shown in Fig. 10, all of the models overestimate the decay rate of III_b; however, the quadratic model does a somewhat better job than the other models. In Figs. 11–13, we consider the experimental data of Le Penven *et al.*[9] pertaining to the case with negative III_b. The phase space portrait of Fig. 11 shows that their experimental data exhibit mild curvature in the ξ-η phase space, which is reproduced by the quadratic model. Figures 12 and 13, which depict the temporal evolution of II_b, show that the Rotta model grossly underpredicts the rate of decay of these quantities. The Lumley model is seen to be somewhat better than the proposed quadratic model in capturing the rapid decay of II_b and III_b in this experiment, where the initial conditions corresponded to $III_b < 0$. Nevertheless it is clear from the results

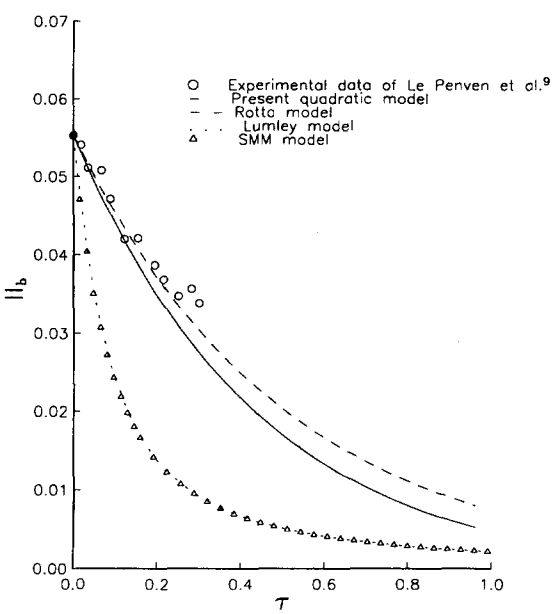

FIG. 9. Temporal decay of the second invariant of the anisotropy tensor: comparison of the model predictions with the plane contraction experiment of Le Penven *et al.*[9] for $III_b(0) > 0$.

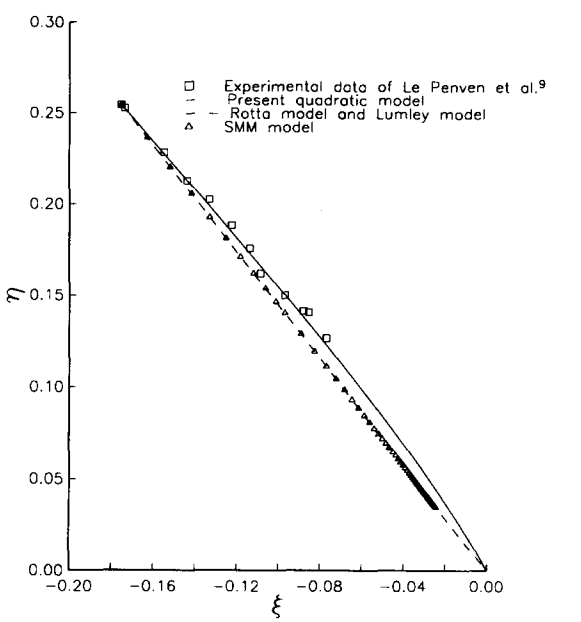

FIG. 11. A phase space comparison of the model predictions with the plane contraction experiment of Le Penven *et al.*[9] for $III_b(0) < 0$.

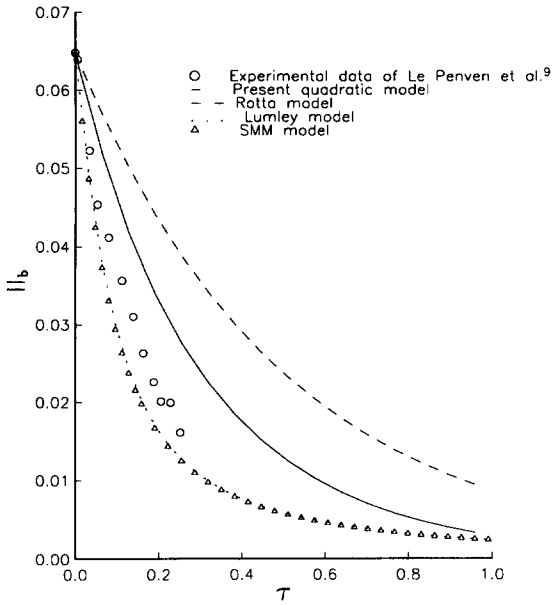

FIG. 12. Temporal decay of the second invariant of the anisotropy tensor: comparison of the model predictions with the plane contraction experiment of Le Penven *et al.*[9] for $III_b(0) < 0$.

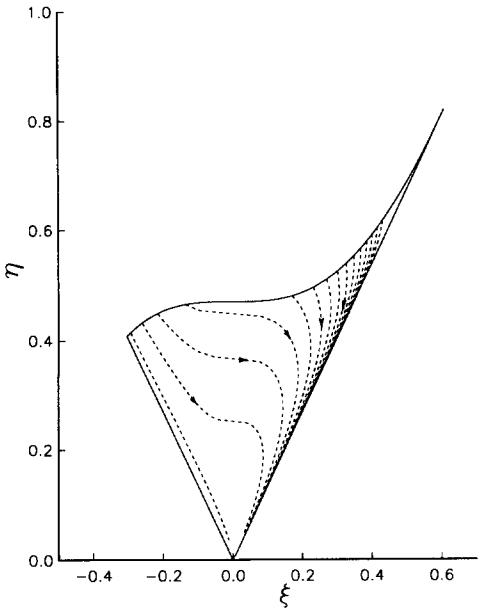

FIG. 14. Trajectories of the quadratic model in ξ-η phase space for a variety of initial conditions.

presented in this section that the quadratic model does the best overall job in predicting the experimental trends. A more elaborate phase space portrait of the quadratic model is shown in Fig. 14, which displays various trajectories of the model with reference to the anisotropy invariant map. These trajectories show the proper trend of a relaxation toward axisymmetry during the return to isotropy process.

VII. CONCLUSION

A quadratic generalization of the linear Rotta model has been developed for the slow pressure-strain correlation of turbulence. This simple nonlinear model, which has only one independent constant, was shown to constitute an improvement on the Rotta model, the quasilinear Lumley model, and the nonlinear SMM model in predicting the trends observed in return to isotropy experiments. Furthermore, for relaxational flows, the quadratic model was shown to satisfy realizability and to have no stable nonzero equilibrium solutions that attract initial conditions which lie in the anisotropy invariant map—a crucial constraint that is necessary to ensure that the model predicts a return to isotropy, independent of the initial conditions. The most notable feature of this new quadratic model is its ability to capture the essence of the return to isotropy problem with a nonlinear structure that is substantially simpler than previously proposed nonlinear generalizations of the Rotta model. The more complicated nonlinear SMM model was found to give essentially the same predictions as the Lumley model for the range of anisotropies and Reynolds numbers studied in the present work. Therefore it may not constitute a significant improvement over the Lumley model which itself does not properly describe highly nonlinear effects. Of course, it should be emphasized that the quadratic model derived in this study (as well as conclusions derived herein), only apply to high Reynolds number turbulent flows.

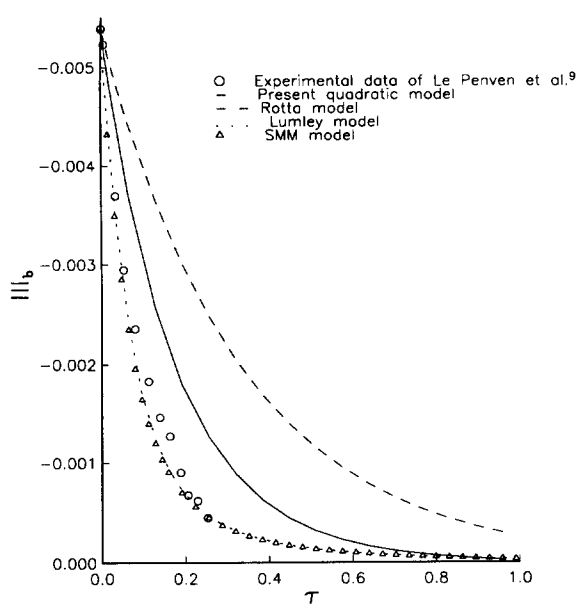

FIG. 13. Temporal decay of the third invariant of the anisotropy tensor: comparison of the model predictions with the plane contraction experiment of Le Penven *et al.*[9] for $III_b(0) < 0$.

Future research can be directed on two fronts: the development of a low turbulence Reynolds number correction of the model and the addition of successively higher-order (for example, cubic) nonlinear terms. Insofar as the former research direction is concerned, the direct numerical simulations of Lee and Reynolds[11] have indicated that history dependent effects of the Reynolds stress and dissipation rate anisotropy tensors are important in low Reynolds number turbulent flows. These are complicating features that are not likely to be described by simple nonlinear models with an algebraic structure. In regard to the addition of higher degree nonlinearities, we feel that it is best to first provide a

systematic test of a quadratic model since second-order closures that are quadratic in the anisotropy tensor can satisfy constraints such as material frame indifference in the limit of two-dimensional turbulence[12,13] and realizability. The satisfaction of these constraints, which are violated by simple second-order closures such as the Launder, Reece, and Rodi model,[7] allow for the description of more complex turbulent flows within the framework of a workable theory. A systematic program for the development of improved second-order closure models that are quadratically nonlinear is currently underway and will be the subject of a future paper.

ACKNOWLEDGMENT

This research was supported by the National Aeronautics and Space Administration under NASA Contract No. NAS1-18605 while the authors were in residence at ICASE, NASA Langley Research Center, Hampton, Virginia 23665.

[1]J. C. Rotta, Z. Phys. **129**, 547 (1951).
[2]J. L. Lumley, Adv. Appl. Mech. **18**, 123 (1978).
[3]J. N. Gence and J. Mathieu, J. Fluid Mech. **101**, 555 (1980).
[4]K. S. Choi and J. L. Lumley, *Proceedings of the IUTAM Symposium, Kyoto, 1983, Turbulence and Chaotic Phenomena in Fluids*, edited by T. Tatsumi (North-Holland, Amsterdam, 1984), p. 267.
[5]T. H. Shih and J. L. Lumley, Cornell University Technical Report No. FDA-85-3, 1985; T. H. Shih, Ph.D. thesis, Cornell University, 1984.
[6]T. H. Shih, N. N. Mansour, and J. Y. Chen, *Center for Turbulence Research, Proceedings of the 1987 Summer Program* (Stanford U.P., Stanford, CA, 1987), p. 191.
[7]B. E. Launder, G. Reece, and W. Rodi, J. Fluid Mech. **68**, 537 (1975).
[8]J. L. Lumley and G. R. Newman, J. Fluid Mech. **82**, 161 (1977).
[9]L. Le Penven, J. N. Gence, and G. Comte-Bellot, in *Frontiers in Fluid Mechanics*, edited by S. H. Davis and J. L. Lumley (Springer, Berlin, 1985), p.1.
[10]S. B. Pope, Prog. Energy Combustion Sci. **11**, 119 (1985).
[11]M. J. Lee and W. C. Reynolds, Stanford University Technical Report No. TF-24, Mechanical Engineering Department, Stanford University, 1985; M. J. Lee, Ph.D. thesis, Stanford University, 1985.
[12]C. G. Speziale, Geophys. Astrophys. Fluid Dyn. **23**, 69 (1983).
[13]C. G. Speziale, Theor. Comput. Fluid Dyn. **1**, 3 (1989).